

# Structural and Ultraviolet-Protective Properties of Nano-TiO<sub>2</sub>-Doped Polypropylene Filaments

Nilüfer Erdem, Umit Halis Erdogan, Aysun Aksit Cireli, Nurhan Onar

Textile Engineering Department, Faculty of Engineering, Dokuz Eylül University, Buca, Izmir, Turkey

Received 15 March 2009; accepted 15 June 2009

DOI 10.1002/app.30950

Published online 27 August 2009 in Wiley InterScience (www.interscience.wiley.com).

**ABSTRACT:** Textiles, with appropriate light absorbers and suitable finishing methods, can be used as ultraviolet (UV) protection materials. In this study, we investigated the effects of nano-TiO<sub>2</sub> particles on the UV-protective and structural properties of polypropylene (PP) textile filaments. Master batches of PP/TiO<sub>2</sub> nanoparticles were prepared by melt compounding before spinning, and filaments incorporating 0.3, 1, and 3% TiO<sub>2</sub> nanoparticles were spun in a pilot melt-spinning machine. The structural properties of the nanocomposite fibers were analyzed with scanning electron microscopy, X-ray diffractometry, differential scanning calorimetry, and tensile tests. The UV-pro-

tection factor was determined to evaluate the UV-protective properties of the filaments. In conclusion, although the structure and mechanical properties of the nanocomposite filaments were slightly affected by the addition of nano-TiO<sub>2</sub>, the UV-protective properties of the PP filaments improved after treatment with nano-TiO<sub>2</sub>, and the nanocomposite filaments exhibited excellent UV protection. © 2009 Wiley Periodicals, Inc. *J Appl Polym Sci* 115: 152–157, 2010

**Key words:** fibers; nanocomposites; poly(propylene); (PP); structure

## INTRODUCTION

Polypropylene (PP) is one of the most widely used thermoplastic polymers in textile and plastic applications. A large variety of PP textile products, such as apparels, coverings, upholstery fabrics, and technical textiles, are available today. Textile products of PP are preferred because of their low cost, easy processing, low density, high tensile strength, and excellent chemical stability. However, there are some disadvantages of PP, such as low polarity, ultraviolet (UV) stability, and thermal stability.<sup>1,2</sup> As a fiber, unstabilized PP is very susceptible to sunlight-initiated deterioration. Therefore, antioxidants and UV stabilizers are required to protect the polymer during use and storage. Although exposure to UV light in the presence of atmospheric oxygen degrades PP fibers, textile products of PP with different UV stabilities and UV blocking properties are available today.

Textiles, with appropriate light absorbers and suitable finishing methods, can be used as UV-protective materials. The use of organic and inorganic par-

ticles as fillers in textiles is one method of modifying these materials for UV protection. Inorganic UV blockers, such as TiO<sub>2</sub>, ZnO, Al<sub>2</sub>O<sub>3</sub>, and SiO<sub>2</sub>, are preferable to organic UV blockers, as they are non-toxic and chemically stable to UV light at high temperatures.<sup>3,4</sup> Among these inorganic UV blockers, TiO<sub>2</sub> and ZnO are commonly used.<sup>5,6</sup>

TiO<sub>2</sub> provides good UV protection by scattering most of the UV rays through its high refractive index and/or by absorbing UV rays because of its semiconductive properties.<sup>4</sup> The wide-band semiconductor TiO<sub>2</sub> exists in three different crystalline polymorphs: rutile, anatase, and brookite. Among them, rutile and anatase are the more common and widely used phases in applications. Although the band gap value is 3.0 eV for the rutile type and 3.2 for the anatase type, they both absorb only UV rays.<sup>7</sup> Furthermore, the development of nanotechnology provides more efficient shielding materials against UV radiation, such as nanoparticles. As the size of particles decreases, their effects increase because of their larger total surface area per unit volume compared to conventional materials.<sup>8,9</sup> Therefore, the number of studies about the modification of the properties of polymeric textile fibers and fabrics by nanoparticles has increased recently.<sup>10–13</sup> In general, two main methods are used to modify textile materials with nanoparticles; the first is the incorporation of the nanoparticles in the textile fibers, and the second is the application of nanoparticles on the textiles during finishing processes. Nanosized TiO<sub>2</sub> has already

Correspondence to: U. H. Erdogan (umit.erdogan@deu.edu.tr).

Contract grant sponsor: Scientific and Technological Research Council of Turkey; contract grant number: TÜB-104M431.

**TABLE I**  
**UPF Classification System of Sun-Protective Textiles**

UPF range	UV radiation protection category	Effective UV radiation transmission (%)	UPF rating
15–24	Good protection	6.7–4.2	15, 20
25–39	Very good protection	4.1–2.6	25, 30, 35
40–50+	Excellent protection	≤2.5	40, 45, 50, 50+

The data were taken from ref. 20.

been applied to fabrics with common coating techniques.<sup>3,10</sup> It has been determined that nanosized TiO<sub>2</sub> is more efficient at absorbing and scattering UV radiation than the conventional size TiO<sub>2</sub> and is thus better able to block UV. Although TiO<sub>2</sub> particles have already been used as a compound of coating material in finishing processes, only a few studies<sup>14,15</sup> have been published on the characterization of fibers modified with TiO<sub>2</sub> nanoparticles. From another point of view, it has already been demonstrated that well-established fiber processing technology can be successfully used to process nanocomposite fibers.<sup>16,17</sup>

In this study, PP textile filaments incorporating 0.3, 1, and 3% TiO<sub>2</sub> nanoparticles were prepared. The structural and the UV-protective properties of these filaments were investigated and are reported.

## EXPERIMENTAL

### Materials

Commercially available TiO<sub>2</sub> spherical nanopowder (Aldrich, Steinheim, Germany) was used in this study. The powder was a mixture of the anatase and rutile phases, and the average particle diameter of the powder was less than 100 nm. An isotactic PP (Ecolen HZ21X, Hellenic Petroleum, Aspropyrgos, Greece) with a melt flow index of 35 g/10 min and a density of 0.90 gr/cm<sup>3</sup> was used to manufacture the filaments.

### Nanocomposite filament spinning

The PP and TiO<sub>2</sub> nanoparticles were mixed by melt compounding with a twin-screw extruder (AB-Tech Scientific, USA) before spinning. Powdered PP and

TiO<sub>2</sub> nanoparticles were dried in a vacuum oven. Before it was fed to the twin-screw extruder, mixtures of PP powder and TiO<sub>2</sub> nanoparticles were prepared, in which the contents of TiO<sub>2</sub> nanoparticles were 0.3, 1, and 3%. The extrusion speed was 60 rpm, and there were six extrusion zones with the temperatures 170, 190, 190, 190, 190, and 195°C. After a defined period of extrusion, the extruded material was cooled in a water bath, pelletized, and cut, and chips (master batch) of the aforementioned concentrations were obtained. A control sample of PP without TiO<sub>2</sub> nanoparticles was also subjected to the same process to obtain a similar thermal history. PP–TiO<sub>2</sub> nanocomposite master batches were converted into filaments with trilobal cross sections with a pilot melt-spinning machine. Melt spinning was carried out on a single-screw extruder (Emerson & Renwick, Ltd., Lancashire, England) with a spinneret containing 40 orifices. The extrusion speed was 15 rpm, and the temperatures in the extrusion zone were 206, 225, 235, 239, and 240°C from the feeder to the spinneret, respectively. The as-spun filaments were subsequently drawn with a draw ratio of 2.5 at 115°C.

### Characterization

The morphological properties of the neat and the composite PP filaments were analyzed with a JEOL (Tokyo, Japan) 6060 scanning electron microscope. The surfaces of the samples were coated with a thin gold layer by a sputtering machine before scanning electron microscopy (SEM) analysis. Longitudinal and cross-sectional SEM images of the samples were obtained.

The structures of the nanocomposite fibers and the control sample were analyzed with X-ray diffraction (XRD) and differential scanning calorimetry

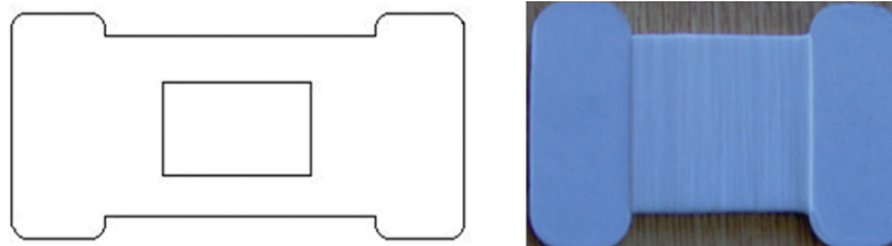


**Figure 1** Sample holder for the PP filaments. [Color figure can be viewed in the online issue, which is available at [www.interscience.wiley.com](http://www.interscience.wiley.com).]

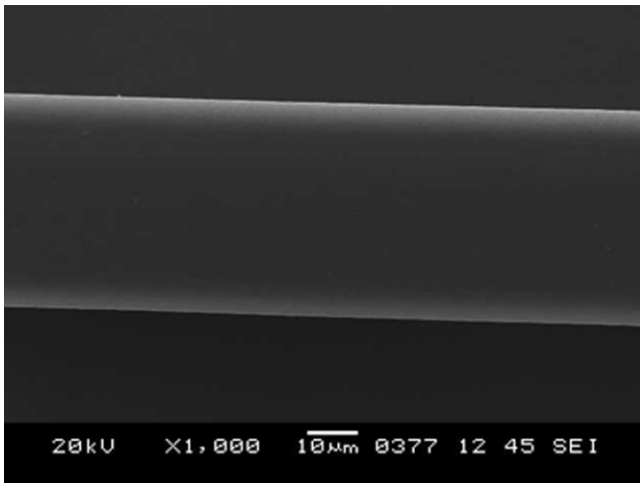


**Figure 2** Longitudinal SEM image of the neat PP.

(DSC). XRD studies were carried out with an XRD Rigaku (Tokyo, Japan) D/Max 2200 PC with Cu  $K\alpha$  radiation at 40 kV and 36 mA. The diffraction angles ( $2\theta$ ) of each sample were measured from 3 to  $90^\circ$  at a scan speed of  $4^\circ/\text{min}$ . DSC measurements were performed on a PerkinElmer/Pyris1 (Beaconsfield, England) in  $N_2$  at a heating and cooling rate of  $20^\circ\text{C}/\text{min}$  in the temperature range  $0\text{--}200^\circ\text{C}$ . The melting temperature ( $T_m$ ) and crystallization temperature ( $T_c$ ) of the samples were obtained by this procedure. The percentage of the crystallinity of the samples was calculated as follows:

$$\text{Crystallinity (\%)} = \frac{\Delta H_f}{\Delta H_f^0} \quad (1)$$

where  $\Delta H_f$  is the enthalpy of fusion of the tested PP fiber samples calculated by division of the endothermic peak area by the weight of PP within the nanocomposite fiber sample and  $\Delta H_f^0$  is the extrapolated

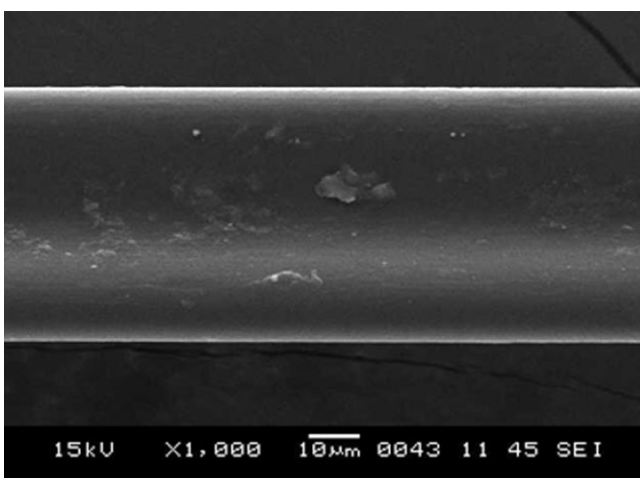


**Figure 3** Longitudinal SEM image of 99.7% PP/0.3% nano-TiO<sub>2</sub>.

value of enthalpy corresponding to the melting of 100% crystalline PP, which was obtained from literature as  $\Delta H_f^0 = 165 \text{ J/g}$ .<sup>18</sup>

The mechanical properties of the fibers were measured with an Instron 4411 (Bucks, England) tensile testing machine equipped with a 10-N cell according to ASTM D 3822-07.<sup>19</sup> The gauge length was 20 mm, and the crosshead speed was 20 mm/min. An average of 25 readings for each fiber sample are reported.

### Analysis of UV-ray transmittance

The sun emits UV radiation in a wavelength range of 100–400 nm, which is conventionally subdivided into three bands: UVA (315–400 nm), UVB (280–315 nm), and UVC (100–280 nm). However, only UV rays with wavelengths of 290–400 nm reach the surface of the earth because UVC and some UVB are absorbed by the stratospheric ozone in the earth's atmosphere.<sup>3,20,21</sup> Exposure to large doses of these solar UV radiations can result in detrimental effects on human skin, including sunburn, premature skin aging, and allergies, if the skin is unprotected.<sup>3,5</sup> As textiles and sun-blocking creams are common choices for shielding against UV radiation, there are detailed procedures involving the UV-protective properties of textiles in various standard methods.<sup>22–24</sup> The term *ultraviolet protection factor* (UPF), which is defined in Australian/New Zealand Standard 4399,<sup>22</sup> has been widely used by the textile and clothing industry to evaluate the UV-protective capacity of textile products.<sup>20</sup> It is defined as follows:<sup>3,21,22</sup>

$$\text{UPF} = \frac{\int_{290}^{400} E_\lambda S_\lambda \Delta\lambda}{\int_{290}^{400} E_\lambda S_\lambda T_\lambda \Delta\lambda} \quad (2)$$

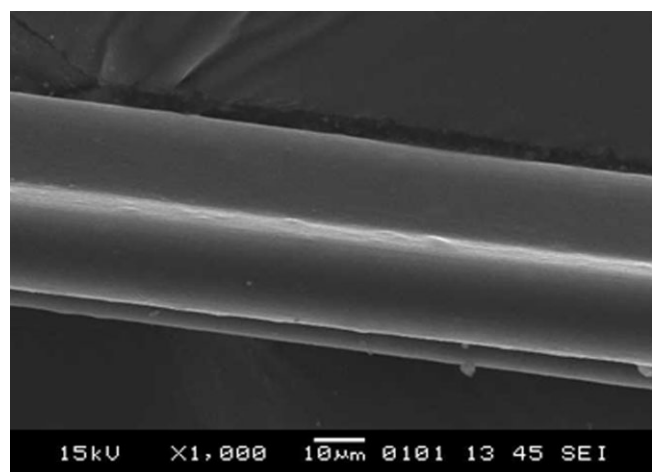


**Figure 4** Longitudinal SEM image of 99% PP/1% nano-TiO<sub>2</sub>.

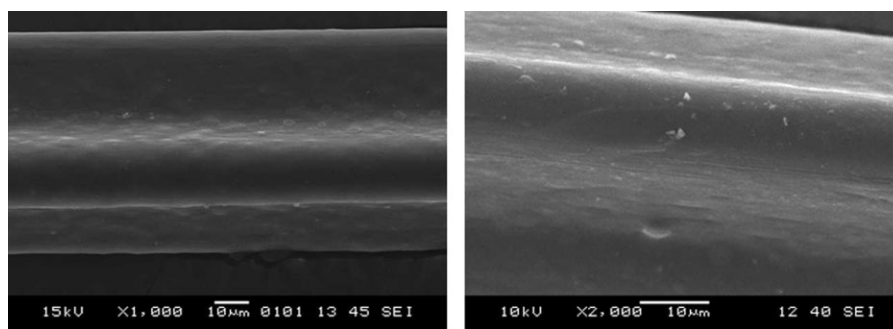


**Figure 5** Longitudinal SEM images of 97% PP/3% nano-TiO<sub>2</sub>.

where  $E_\lambda$  is the relative erythemal spectral effectiveness,  $S_\lambda$  is the solar UV spectral irradiance,  $T_\lambda$  is the spectral transmittance of the specimen (incoming light that passes through the specimen),  $\Delta\lambda$  is the wavelength increment (nm), and  $\lambda$  represents the wavelength (nm). When  $\Delta\lambda$  is constant, two more indices can be calculated by

$$T_{\text{UVA}} = \frac{1}{m} \sum_{315}^{400} T_\lambda, T_{\text{UVB}} = \frac{1}{n} \sum_{290}^{315} T_\lambda \quad (3)$$

where  $T_{\text{UVA}}$  and  $T_{\text{UVB}}$  (%) are the means of transmittance under UVA and UVB, respectively, and  $m$  and  $n$  are the numbers of measurement points for UVA and UVB, respectively.<sup>3,20,21</sup>

The Australian/New Zealand standard also indicates a classification system of the textiles according to their sun-protective properties. For the purposes of labeling, sun-protective textiles should be categorized according to their rated UPF, as shown in Table I. The rated UPF will always be a value that is a multiple of 5. For UPF ratings of 51 or greater, the term 50+ is used.<sup>20,21</sup>

In this study, an SDL Atlas Camspec M350 ultraviolet-visible spectrophotometer (Stockport, England) was used to characterize UV-protective properties. The samples were placed in a spectrophotometer and scanned between 290 and 400 nm with a 5-nm interval at room temperature. A special sample holder was chosen to carry out the tests. The sample holder was a cardboard piece that had a rectangular hole in its center (Fig. 1). The filaments were wrapped in an orderly manner around the hole, which resembled a fabric, with a simple winding machine before the test. Consequently, the aforementioned method enabled us to evaluate the UV-protective properties of the filaments before fabrication.

## RESULTS AND DISCUSSION

### Morphological properties

The longitudinal SEM micrographs of the neat PP and PP/TiO<sub>2</sub> nanocomposite filaments with differ-

ent TiO<sub>2</sub> contents are shown in Figures 2–5. The surfaces of the filaments were investigated in terms of their shape and uniformity. Clearly, the neat PP showed the smoothest surface in comparison to the nanocomposite filaments. Fibers filled with nano-TiO<sub>2</sub> particles had some surface irregularities as the amount of nanoparticle increased. These surface protrusions of the fibers were most probably due to nanoparticle agglomeration. It is also evident from the figures that the agglomerates were discontinuous throughout the fiber. The nanocomposite of 3% TiO<sub>2</sub> contained more agglomerates or larger particles than the other nanocomposite filaments. The cross section of the nanocomposite filament including 3% TiO<sub>2</sub> is given in Figure 6. The cross section of the fiber was uniform and smooth. Consequently, the surface SEM micrographs of the PP/TiO<sub>2</sub> nanocomposite fibers showed a number of irregularities throughout the fiber due to nanoparticle agglomeration. Therefore, as the content of particles increased, their distribution became nonhomogeneous. However, no inhomogeneity was observed in the cross-sectional images of the fibers.

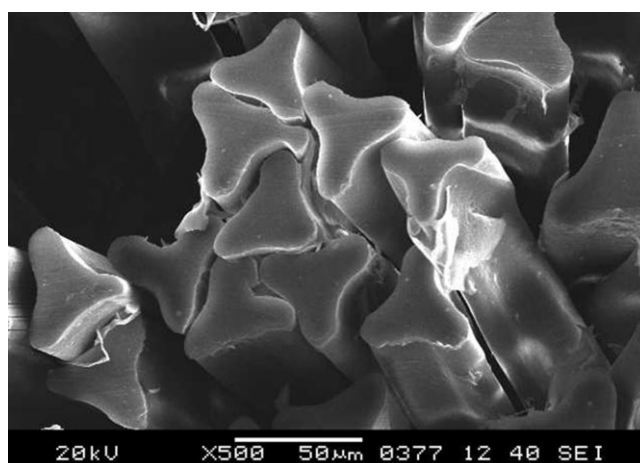


**Figure 6** Cross-sectional SEM image of the nanocomposite fibers (97% PP/3% nano-TiO<sub>2</sub>).

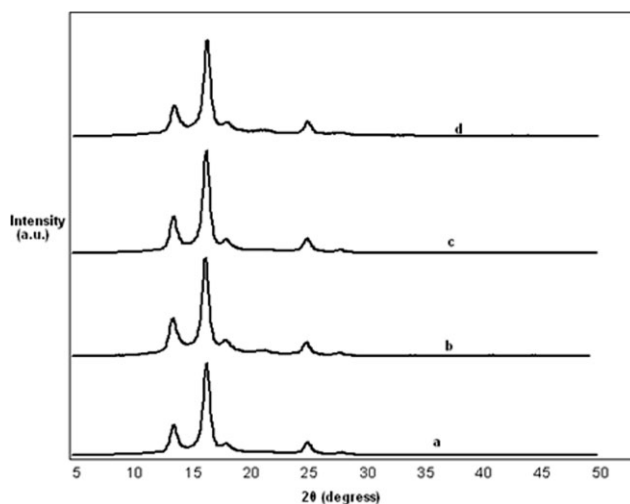


**Figure 7** XRD patterns of the fibers: (a) neat PP, (b) 99.7% PP/0.3% nano-TiO<sub>2</sub>, (c) 99% PP/1% nano-TiO<sub>2</sub>, and (d) 97% PP/3% nano-TiO<sub>2</sub>.

### Structural and thermal properties

Figure 7 illustrates the integrated XRD patterns of the nanocomposite fibers with different TiO<sub>2</sub> contents. The diffraction peaks of the PP crystals, which ranged from 10 to 30°, indicated a typical  $\alpha$  form of PP crystals. Because of the high speed of the extrusion line in filament spinning, the formation of the  $\beta$  -form crystalline structure was overruled.<sup>1,25</sup> As shown in Figure 7, the diffraction pattern of PP crystals did not indicate any significant change. However, the degree of crystallinity (the intensity and height of peaks) changed slightly with respect to nanoparticle content.

The crystallization and melting characteristics of the filaments are presented in Table II. Only minor differences were observed in  $T_c$  and percentage crystallinity. The degree of crystallinity of PP enhanced by the addition of nano-TiO<sub>2</sub> was close to that of neat PP. The crystallinity increased slightly up to 56.4% in the presence of 0.3% TiO<sub>2</sub>; however, the crystallinity decreased to 54.5% as the filler content increased up to 3%. These findings were most probably due to the nucleation role of nano-TiO<sub>2</sub> in the crystallization of PP, which resulted in a higher degree of crystallinity and a higher  $T_c$ . However, we also concluded that larger aggregates prevented

**TABLE II**  
Crystallization and Melting Characteristics of the Fibers

Content of nano-TiO <sub>2</sub> (%)	$T_c$ (°C)	$T_m$ (°C)	Crystallinity (%)
0	112.97	164.29	53.4
0.3	112.10	164.50	56.4
1	113.50	164.50	54.7
3	113.10	164.50	54.5

**TABLE III**  
Mechanical Properties of the Fibers

Content of nano-TiO <sub>2</sub> (%)	Tensile strength (g/denier)	Elongation (%)
0	2.43	319.00
0.3	2.23	309.20
1	2.45	302.60
3	2.31	302.11

crystal growth and, hence, reduced the crystallinity as the nano-TiO<sub>2</sub> content increased up to 1 and 3%. Because the addition of nanoparticles was not expected to affect the molecular weight or to cause any chain branching in PP, only the nucleating activity of the nanoparticles was considered. Table II also shows that  $T_m$  remained somewhat unchangeable.

### Mechanical properties

The mechanical properties of the fibers were measured to evaluate the effect of the nanoparticles on the fiber properties. As shown in Table III, there were only small differences found in terms of the tensile strength and elongation. The nanoparticles could act as nucleating centers of crystallization and influence the mechanical properties. In addition, the particles could prevent cohesive interactions and reduce the mechanical properties.

### UV-protective properties

The mean UVA and UVB (effective UV transmission) and UPF values of the PP/TiO<sub>2</sub> nanocomposite filaments are given in Table IV. As the result of treatment with nano-TiO<sub>2</sub>, UPF values of the PP filaments increased significantly from 5 to 50+. The UPF values for all filaments containing nano-TiO<sub>2</sub> exceeded 50. Therefore, the nanocomposite filaments could be labeled as *excellent protective* according to the UPF classification system shown in Table I. In the case of the neat PP filament, a low UPF rating of 5, which was classified as nonrateable, was measured. It was also apparent that the mean UVA and the mean UVB of the PP/TiO<sub>2</sub> nanocomposite filaments were all smaller than those of the neat PP filament. The effective UV transmissions of neat PP were 18 and 13.5% in the UVA and UVB regions,

**TABLE IV**  
UV-Protective Properties of the Samples

Content of nano-TiO <sub>2</sub> (%)	UPF	T_UVA (%)	T_UVB (%)
0	5	18	13.9
0.3	50+	1	0.8
1	50+	0.5	0
3	50+	0	0

respectively. When a low nano-TiO<sub>2</sub> amount (0.3%) was added to PP, the transmittance of filaments in the UVA region sharply decreased from 18 to 1%. A similar trend was also observed in the UVB region.

### CONCLUSIONS

In this study, nanocomposite filaments were prepared with PP and nano-TiO<sub>2</sub> particles with a pilot melt-spinning machine to obtain UV-protective yarns for textiles. Although some protrusions, agglomerations, and nonhomogeneous dispersions of nanoparticles were observed on the surface of the nanocomposite filaments, no inhomogeneities occurred in the cross-sectional shapes of the fibers. As shown by the XRD peaks, the typical  $\alpha$  form of the PP crystals were observed for all filaments. However, the degree of crystallinity changed ambiguously with respect to the content of nano-TiO<sub>2</sub> particles because of particle agglomerations. The crystalline peak temperatures of the fibers rose slightly with increasing content of nano-TiO<sub>2</sub> particles because of their nucleating effect. With regard to the mechanical properties, there were only small differences found. The UV-protective properties of the nanocomposite filaments improved by means of all three indices. The UPF values for the all of filaments containing TiO<sub>2</sub> exceeded 50. The UVA and UVB transmittances of the PP/TiO<sub>2</sub> nanocomposite filaments were all smaller than those of the neat PP filament. The nanocomposite filaments exhibited excellent UV protection.

Consequently, the structural and mechanical properties of the nanocomposite filaments including 0.3, 1, and 3% TiO<sub>2</sub> nanoparticles did not change significantly. On the other hand, the effective UV transmissions of the filaments improved greatly in the presence of the TiO<sub>2</sub> nanoparticles. These findings indicated that TiO<sub>2</sub> nanoparticles improved the UV-blocking properties of the PP filaments remarkably, although some TiO<sub>2</sub> nanoparticles aggregated in the polymer. However, further work is needed to decrease agglomeration with the retention of the mechanical and UV performances.

The authors thank Clariant Turkey (Masterbatches Division) and Renkplast Plastic, Ltd., for their technical support and assistance.

### References

1. Zhu, M. F.; Yang, H. H. In *Handbook of Fiber Chemistry*, 3rd ed.; Lewin, M., Ed.; CRC: New York, 2006; Chapter 3, p 139.
2. Qian, G.; Lan, T. In *Handbook of Polypropylene and Polypropylene Composites*; Harutun, G. K., Ed.; Marcel Dekker: New York, 2003; Chapter 20, p 707.
3. Yang, H.; Zhu, S.; Pan, N. *J Appl Polym Sci* 2004, 92, 3201.
4. Wong, Y. W. H.; Yuen, C. W. M.; Leung, M. Y. S.; Ku, S. K. A.; Lam, H. L. I. *Autex Res J* 2006, 6, 1.
5. Xin, J. H.; Daoud, W. A.; Kong, Y. Y. *Text Res J* 2004, 74, 97.
6. Saito, M. *J Coated Fabrics* 1993, 23, 150.
7. Amemia, S. *Three Bond Tech News* 2004, 62, 1.
8. Schadler, L. S. In *Nanocomposite Science and Technology*; Ajayan, P. M.; Schadler, L. S.; Braun, P. V., Eds.; Wiley-VCH: Weinheim, 2003; Chapter 2, p 77.
9. Hussain, F.; Hojjati, M.; Okamoto, M.; Gorga, R. E. *J Compos Mater* 2006, 40, 1511.
10. Han, K.; Yu, M. *J Appl Polym Sci* 2006, 100, 1588.
11. Erdem, N.; Cireli, A. A.; Erdogan, U. H. *J Appl Polym Sci* 2009, 111, 2085.
12. Rottstegge, J.; Qiao, Y. K.; Zhang, X.; Zhou, Y.; Xu, D.; Han, C. C.; Wang, D. *J Appl Polym Sci* 2007, 103, 218.
13. Catone, D. L. *Chem Fibers Int* 2004, 54, 25.
14. Huang, Y.; Chen, T.; Tang, J.; Yeh, C.; Tien, C. *Ind Eng Chem Res* 2007, 46, 5548.
15. Dastjerdi, R.; Mojtahedi, M. R. M.; Shoshtari, A. M. *Macromol Symp* 2008, 274, 154.
16. Chatterjee, A.; Deopura, B. L. *Compos A* 2006, 37, 813.
17. Kumar, S.; Doshi, H.; Srinivasarao, M.; Park, J. O.; Schiraldi, D. A. *Polymer* 2002, 43, 1701.
18. Wunderlich, B. *Macromolecular Physics*; Academic: New York, 1960; Vol. 3, p 48.
19. ASTM D 3822-07: Standard Test Method for Tensile Properties of Single Textile Fibers; ASTM International: West Conshohocken, PA, 2007.
20. Algaba, I.; Riva, A. *Color Technol* 2002, 118, 52.
21. Algaba, I.; Riva, A.; Pepio, A. *Text Res J* 2007, 77, 826.
22. AS/NZS 4399-1996: Sun Protective Clothing Evaluation and Classification; Standards Australian/Standards New Zealand, Sydney, Wellington, New Zealand, 1996.
23. AATCC Test Method 183-1998: Transmittance of Blocking of Erythemally Weighted Ultraviolet Radiation Through Fabrics; American Association of Textile Chemists and Colorists: Research Triangle Park, NC, 2004.
24. EN 13758-1: Textiles—Solar UV Protective Properties—Part 1: Method of Test for Apparel Fabrics; CEN: Brussels, 2001.
25. Everaert, R. *Chem Fibers Int* 2004, 54, 192.